



Published in final edited form as:

Mol Cancer Ther. 2020 November ; 19(11): 2330–2339. doi:10.1158/1535-7163.MCT-20-0407.

LILRB4-Targeting Antibody–Drug Conjugates for the Treatment of Acute Myeloid Leukemia

Yasuaki Anami^{a,†}, Mi Deng^{b,†}, Xun Gui^{a,†}, Aiko Yamaguchi^a, Chisato M. Yamazaki^a, Ningyan Zhang^a, Cheng Cheng Zhang^b, Zhiqiang An^a, Kyoji Tsuchikama^a

^aTexas Therapeutics Institute, The Brown Foundation Institute of Molecular Medicine, The University of Texas Health Science Center at Houston, 1881 East Road, Houston, TX 77054

^bDepartment of Physiology, The University of Texas Southwestern Medical Center, 6001 Forest Park Road, Dallas, TX 75390

Abstract

Acute myeloid leukemia (AML) is the most common and aggressive blood cancer in adults. In particular, significant unmet medical needs exist for effective treatment strategies for M4 and M5 AML subtypes. Antibody-drug conjugates (ADCs) are a promising drug class for AML therapy, as demonstrated by the FDA-approved anti-CD33 ADC gemtuzumab ozogamicin (Mylotarg[®]). However, CD33 is expressed in normal hematopoietic stem cells, highlighting the critical need to identify AML-specific targets to minimize the risk of potential adverse effects. We have demonstrated that the leukocyte immunoglobulin-like receptor subfamily B4 (LILRB4) is expressed at significantly higher levels on monocytic M4 and M5 AML cells than on normal counterparts. Here, we test whether LILRB4 is a promising ADC target to kill monocytic AML cells while sparing healthy counterparts. To this end, we generated ADCs from a humanized anti-LILRB4 monoclonal antibody and the antimitotic payload monomethyl auristatin F (MMAF). The conjugates constructed were characterized and evaluated for LILRB4-specific cell killing potency, toxicity to progenitor cells, pharmacokinetics, and therapeutic efficacy. Our ADC linker technology platform efficiently generated homogeneous anti-LILRB4 ADCs with defined drug-to-antibody ratios. The homogeneous anti-LILRB4 ADCs demonstrated the capacity for LILRB4-mediated internalization, suitable physicochemical properties, and high cell killing potency against LILRB4-positive AML cells. Importantly, our data indicate that these ADCs spare normal progenitor cells. One of our homogeneous conjugates exerts a remarkable therapeutic effect and no significant toxicity in a xenograft mouse model of disseminated human AML. Our findings highlight the clinical potential of anti-LILRB4 ADCs in monocytic AML therapy.

Corresponding Authors: Cheng Cheng Zhang, Department of Physiology, The University of Texas Southwestern Medical Center, 6001 Forest Park Road, Dallas, TX 75390 (Alec.Zhang@UTSouthwestern.edu), Zhiqiang An, Texas Therapeutics Institute, The Brown Foundation Institute of Molecular Medicine, The University of Texas Health Science Center at Houston, 1881 East Road, Houston, TX 77054 (Zhiqiang.An@uth.tmc.edu), Kyoji Tsuchikama, Texas Therapeutics Institute, The Brown Foundation Institute of Molecular Medicine, The University of Texas Health Science Center at Houston, 1881 East Road, Houston, TX 77054 (Kyoji.Tsuchikama@uth.tmc.edu).

[†]These authors contributed equally.

Introduction

Acute myeloid leukemia (AML) is the most common acute leukemia in adults and a common pediatric cancer. Despite treatment, most patients relapse and succumb to disease within 5 years. Monocytic AML, including acute myelomonocytic leukemia (M4) and acute monocytic leukemia (M5), accounts for approximately 30% of all cases of AML(1). AML patients with a significant monocytic component are more likely to have evidence of extramedullary disease(1) and hyperleukocytosis(2), which is associated with a poor prognosis. In addition, clinical studies suggest that monocytic AML carries a greater risk for marrow and extramedullary relapse after stem cell transplant compared with non-monocytic subtypes(3).

The FDA has recently approved several new drugs for AML targeting CD33, isocitrate dehydrogenase 1 (IDH1), IDH2, FMS-like tyrosine kinase 3 (Flt3), BCL-2, and hedgehog(4). The BCL-2 inhibitor venetoclax along with azacytidine is an emerging standard of care for patients over 65 years of age and patients with comorbid conditions precluding intensive chemotherapy(5). However, a recent report demonstrates that the M5b subtype (acute monoblastic leukemia) is associated with resistance to venetoclax(6). The IC₅₀ for venetoclax is significantly higher in acute monoblastic leukemia than in other AML subtypes. Thus, there is a significant unmet medical need for effective treatment strategies for monocytic AML, particularly M4 and M5 subtypes that are associated with high risks for relapse after stem cell transplant and resistance to current therapies.

Antibody-drug conjugates (ADCs) are emerging chemotherapeutic agents for treating cancers including AML(7). ADCs consist of monoclonal antibodies (mAbs) conjugated with cytotoxic agents (payloads) through stable chemical linkers. Properly designed ADCs can selectively deliver payloads to target tumor cells, resulting in improved potency, broad therapeutic window, and prolonged circulation life compared to conventional drug classes for chemotherapy. Eight ADCs have been approved by the FDA and more than 100 ADCs are currently in clinical trials. Gemtuzumab ozogamicin (Mylotarg®) is the first ADC approved for the treatment of newly diagnosed or refractory CD33-positive AML(8). While promising, Mylotarg® was originally withdrawn from the market in 2010 due to unexpected safety issues. It was re-approved in 2017 for patients with relapsed or refractory CD-33 positive AML with a lower dose and a modified schedule(9). CD33 is expressed not only in AML blasts but also in normal hematopoietic stem cells (HSCs)(10). This lack of specificity likely contributes to the narrow therapeutic window of any anti-CD33 agents. Several other AML receptors, including CD123(11) and C-type lectin-like molecule-1 (CLL-1)(12), are being tested as ADC targets. However, CD33 is the sole target that has been clinically validated so far for AML therapy using ADCs.

Another concern with Mylotarg® is its heterogeneous molecular composition. Mylotarg® is prepared by stochastic lysine coupling, yielding a heterogeneous mixture of conjugates that differ in conjugation site and drug-to-antibody ratio (DAR). Heterogeneous antibody–drug conjugation can lead to poor pharmacokinetics (PK), efficacy, and safety profiles(13). Collectively, ADCs targeting AML-specific antigens highly likely lead to more effective AML therapy with broader therapeutic indices than does Mylotarg®. Ideally, such ADCs

should be prepared by site-specific antibody-drug conjugation to overcome the issues associated with ADC heterogeneity. So far, a few ADCs including SGN-CD123A(14) and IMG632(11) have been developed based on these molecular design strategies.

The leukocyte immunoglobulin-like receptor subfamily B (LILRB) is a group of type I transmembrane glycoproteins expressed by normal and malignant human cells of the myelomonocytic origin(15). Because of the negative roles of phosphatases in immune activation, LILRBs are considered to be immune checkpoint factors(16). The most restrictively expressed member of the LILRB family is LILRB4. LILRB4 is expressed on normal monocytic cells (monocytes, macrophages, and some dendritic cells)(15) and to a lesser extent on plasmablasts(17). LILRB4 is not expressed on neutrophils, other myeloid cells, or hematopoietic stem or progenitor cells (HSPCs)(18). LILRB4 is expressed at significantly higher levels on monocytic AML cells than on normal counterparts, and its level inversely correlates with overall survival of patients with AML(18–20). Importantly, we have discovered that LILRB4 supports tumor development by facilitating leukemia cell infiltration into tissues and by suppressing T cell activity through the ApoE/LILRB4/SHP2/NF κ B/uPAR/ARG1 axis in AML cells(19). Furthermore, we have studied anti-LILRB4 blocking antibodies and CAR-T cells that can efficiently inhibit AML development in various mouse models including humanized and patient-derived xenografted mice(18,19). LILRB4 thus represents an attractive target for treating monocytic AML to achieve effective and safe targeted therapy.

Here, we show that the branched linker(21–24) and glutamic acid-valine-citrulline linker technologies(25) developed by our group efficiently provide anti-LILRB4 ADCs with high homogeneity, desirable physicochemical properties, high cell killing potency against AML cells, and marginal toxicity to normal progenitor cells. We also demonstrate that our conjugates exert a significant therapeutic effect in a mouse model of disseminated human AML. Our findings highlight the clinical potential of our anti-LILRB4 ADCs in AML therapy.

Materials and Methods

Preparation of human mAbs with an N297A or N297Q mutation

We expressed the humanized anti-LILRB4 mAb h128–3 (IgG1, wild-type) as previously described(26). Site-directed mutagenesis was performed to make N297A and N297Q Fc variants. The N297A variant mAb contains an alanine (A) at the amino acid residue 297 (European numbering system) in the CH2 region of the wild-type h128–3 heavy chain. The N297Q variant mAb contains a glutamine (Q) at this position. The constructs for the mutated heavy chain and wild-type light chain were co-transfected into human embryonic kidney freestyle 293 cells (HEK293F, ThermoFisher) using polyethyleneimine (PEI, Sigma) as a transfection reagent. Seven days after co-transfection, supernatants were harvested and antibodies were purified by affinity chromatography using protein A resin (Repligen) as reported previously.

Cell lines

Human monocytic AML cell lines THP-1 (TIB-202), MV4–11 (CRL-9591), and U937 (CRL-1593.2) were purchased from ATCC within the period of 2010 to 2018, characterized by the vendor using routine DNA profiling, and no further authentication was conducted by the authors. All cell lines were routinely tested using a mycoplasma-contamination kit (R&D Systems) to make sure no contamination in cell cultures and passaged before becoming fully confluent up to 20 passages.

LILRB4 internalization assay

THP-1 or MV4–11 cells were seeded in 24-well plates (5×10^4 cells/well, 1 mL) and incubated with N297A and N297Q Fc variants (5 $\mu\text{g}/\text{mL}$) at 37 °C for 24 h. Subsequently, cells were blocked with 300 $\mu\text{g}/\text{mL}$ human IgG (generated in-house) at 4 °C for 1 h. Finally, surface LILRB4 was stained with a non-competitive rabbit anti-LILRB4 antibody R193 (5 $\mu\text{g}/\text{mL}$, generated in-house), incubated with 1/200 diluted 488-conjugated goat F(ab')₂ anti-rabbit F(ab')₂ (Jackson ImmunoResearch Laboratories), and quantified by FACS. The degree of internalization was calculated by dividing the signal from the sample treated with anti-LILRB4 antibodies by the signal from the sample treated with PBS. This value was expressed as a percentage.

MTGase-mediated antibody–linker conjugation

Anti-LILRB4 IgG1 with a N297A or N297Q mutation or an in house-generated isotype control (330 μL in PBS, 17.2 mg/mL, 5.68 mg antibody) was incubated with a diazidoamine branched linker(21,22) (30.3 μL of 100 mM stock in water, 80 equiv.) and Activa TI® (90 μL of 40% w/v solution in PBS, Ajinomoto, purchased from Modernist Pantry) at room temperature overnight. The reaction was monitored by LC-MS equipped with a MabPac RP column (3 \times 50 mm, 4 μm , Thermo Scientific). Elution conditions were as follows: mobile phase A = water (0.1% formic acid); mobile phase B = acetonitrile (0.1% formic acid); gradient over 6.8 min from A:B = 75:25 to 1:99; flow rate = 0.4 mL/min. The conjugated antibodies were purified by SEC (Superdex 200 increase 10/300 GL, GE Healthcare, solvent: PBS, flow rate = 0.6 mL/min) to afford pure, monomeric, and homogeneous antibody-linker conjugates (5.50 mg, >95% yield determined by bicinchoninic acid (BCA) assay).

Strain-promoted azide–alkyne cycloaddition for payload installation

DBCO–peg₃–EVCit–PABC–MMAF (44.0 μL of 4 mM stock solution in DMSO, 1.5 equivalent per azide, synthesized according to our previous report(25) was added to a solution of each mAb–linker conjugate in PBS (840 μL , 5.2 mg/mL). The mixture was incubated at room temperature for 2 h. The reaction was monitored by LC-MS equipped with a MabPac RP column and the crude products were purified by SEC. Anti-LILBR4 and non-targeting ADCs with a DAR of 4 were obtained from the corresponding N297A-linker conjugates; anti-LILRB4 ADCs with a DAR of 8 were obtained from the N297Q mAb–linker conjugate (>95% yield in both cases, determined by BCA assay). Analysis and purification conditions were the same as described above. Average DAR values were determined by reverse-phase HPLC (based on UV peak areas at 280 nm). Non-targeting

ADCs were prepared in the same manner. Purified ADCs were formulated in PBS or citrate buffer (20 mM sodium citrate and 1 mM citric acid, pH 6.6) containing 0.1% Tween 80 and trehalose (70 mg/mL) and stored at 4 °C until use (for up to a month).

Long-term stability test

Each ADC (1 mg/mL, 100 µL) in PBS was incubated at 37 °C. An aliquot (10 µL) was taken after 28 days and analyzed using an Agilent 1100 HPLC system equipped with a MAbPac SEC-1 analytical column (4.0×300 mm, 5 µm, Thermo Scientific). The conditions were as follows: solvent = PBS; flow rate = 0.2 mL/min.

Hydrophobic interaction chromatography analysis

Each ADC (1 mg/mL, 10 µL in PBS) was analyzed using an Agilent 1100 HPLC system equipped with a MAbPac HIC-Butyl column (4.6×100 mm, 5 µm, Thermo Scientific). Elution conditions were as follows: mobile phase A = 50 mM sodium phosphate containing ammonium sulfate (1.5 M) and 5% isopropanol (pH 7.4); mobile phase B = 50 mM sodium phosphate containing 20% isopropanol (pH 7.4); gradient over 30 min from A:B = 99:1 to 1:99; flow rate = 0.5 mL/min.

ELISA binding assay

Corning 96-well EIA/RIA plates were coated overnight at 4°C with human LILRB4 recombinant protein (rhLILRB4-his, 1 µg/mL, Sino Biologicals) and blocked for 2 h at 37 °C with 5% non-fat milk. Serial dilutions of anti-LILRB4 antibodies (h128–3-N297A mAb, DAR-4 ADC, DAR-8 ADC, and hIgG isotype control, 100 µL each) were added and incubated for 2 h at room temperature. Subsequently, the plates were washed with PBS-Tween 20 (0.05%) three times and then incubated for 1 h with HRP-conjugated anti-hFc antibody (Jackson ImmunoResearch Laboratories) at room temperature. Finally, TMB substrate (Sigma) was added to each well. Color development was stopped with 2 M sulfuric acid and absorbance in each well (450 nm) was recorded using a plate reader (Molecular Devices).

Cell viability assay

THP-1, MV4–11, and U937 cells were cultured in Roswell Park Memorial Institute (RPMI) 1640 supplemented with 10% FBS at 37 °C under 5% CO₂ and atmospheric O₂ levels. To test the effects of ADCs on cell growth, 5,000 cells were cultured in each well of 96-well plate and treated with indicated drugs or ADCs for 5 days. Propidium iodide (10 µg/mL) was added to the treated cells and then live cells (Propidium iodide-negative) were counted using a flow cytometer (FACSCalibur, BD Biosciences, CA). EC₅₀ values were determined by non-linear curve fitting (4-variable parameters) using Graphpad Prism 8 software.

Colony-forming unit (CFU) assay

Human umbilical cord blood CD34⁺ cells (Stemcell Technologies, Catalog #: 70008.5) or THP-1 cells (400 cells each) were treated with serial diluted concentrations of an indicated mAb or ADC, and resuspended in MethoCult Classic (Stemcell, Cat#4434), plated, and

incubated in a humidified chamber per manufacturer's directions. Colonies were classified and counted after 8 days.

In vivo PK study

Animal work described in this manuscript was approved and conducted under the oversight of the UT Southwestern (UTSW) Institutional Animal Care and Use Committee. In each study, age-matched (4–8 weeks) female mice were used and randomly allocated to each group. The minimum number of mice in each group was calculated based on the results from our prior relevant studies(19). NOD-scid IL2R γ null (NSG) mice were purchased from and maintained at the animal core facility of UTSW. NSG mice were injected intravenously with 1×10^6 human leukemia cells on Day 0 and 30 mg/kg of normal human IgG (Innovative Research) for preconditioning on Day 6. Low doses of antibody-based therapeutics in mice lacking endogenous antibodies reportedly suffered from a severely impaired half-life in circulation(27). Preconditioning using IgG has been established as a means to overcome this issue in NSG mice. On Day 7, animals were injected with a single dose of unconjugated mAb or ADCs (3 mg/kg) via the tail vein. Blood samples were collected into tubes at 15 min, 6 h, 24 h, 48 h, 96 h, 216 h, and 336 h after injection (5 animals/time point). After being centrifuged at $1,500 \times g$ for 10 minutes, plasma fractions were transferred to sterile cryovials, aliquoted, and stored at -80°C until analysis. Plasma concentrations of anti-LILRB4 mAb and MMAF ADCs were determined by ELISA. Antibody and ADCs in the diluted plasma samples were captured on ELISA plates precoated with LILRB4 recombinant protein (2 $\mu\text{g}/\text{mL}$) for total anti-LILRB4 antibody detection or anti-MMAF polyclonal antibodies (1 $\mu\text{g}/\text{mL}$, Levena Biopharma) for intact ADC detection. Alkaline phosphatase-conjugated goat anti-human IgG F(ab) $_2$ (Jackson ImmunoResearch Laboratories) was used as detection antibody with 1:5000 dilution. Fluorescence signals were developed with a substrate solution of 4-MUP (Sigma) and recorded using a microplate reader (excitation: 340 nm, emission: 460 nm). AUC was calculated using Graphpad Prism 8 software.

In vivo treatment study

Xenografted mice were prepared essentially as described above. Briefly, 6–8 week-old NSG mice were used for transplantation. THP-1 cells stably expressing luciferase(19) (1×10^6 cells) were resuspended in 200 μl PBS for each mouse. All mice were preconditioned with 30 mg/kg human IgG (i.v.) 24 h before ADC injection. Subsequently, mice were given the ADC drugs indicated or control IgG intravenously at day 7, 14, and 21 post transplantation. Leukemia growth was monitored by bioluminescence imaging using an IVIS in vivo imager (Max, 3×10^8 p/sec/cm 2 /sr; Min, 5×10^6 p/sec/cm 2 /sr). Bioluminescence imaging and body weight measurement were performed every 3 or 4 days. All animals were monitored daily and deaths were recorded when moribund animals were euthanized or found dead. Kaplan-Meier survival curve statistics were analyzed using the log-rank (Mantel–Cox) test.

Results

Construction and characterization of anti-LILRB4 ADCs

Receptor-mediated internalization is a key mechanism by which ADCs exert a cytotoxic effect upon intracellular release of payloads. We sought to test whether the anti-LILRB4 mAb h128–3 with a N297A- or N297Q-Fc mutation could internalize upon binding to LILRB4 on leukemia cells. Toward this end, we quantified LILRB4 expressed on the surface of THP-1 and MV4–11 cells before and after being treated with these antibodies or an isotype control for 24 h (Fig. 1). The surface LILRB4 levels were consistent at 4 °C in either case (Fig. S1). However, the surface LILRB4 levels decreased after incubation with either N297A or N297Q mAb at 37 °C for 24 h, indicating that these mAbs were internalized. The observed time- and temperature-dependent internalization indicates that binding of these mAbs to LILRB4 triggers receptor-mediated endocytosis(28). The non-targeting control was not efficiently internalized into either cell type even at elevated temperature.

Based on the findings above, we set out to generate LILRB4-targeting ADCs from these mAbs using the homogeneous antibody–drug conjugation technologies developed by our group(21,22) (Fig. 2A). First, we introduced branched diazidoamine linkers onto the Fc variants of h128–3 mAb at glutamine 295 (Q295) by microbial transglutaminase (MTGase)-mediated conjugation. The branched linker was also introduced at Q297 in the case of the mAb with a N297Q mutation. This high-yielding conjugation provided homogeneous mAb–branched linker conjugates from both Fc variants. Subsequently, we installed the antimitotic agent monomethyl auristatin F (MMAF) onto the linker conjugates by strain-promoted azide–alkyne click reaction. To this end, we used a payload module consisting of dibenzocyclooctyne (DBCO), polyethylene glycol (PEG) spacer, glutamic acid–valine–citrulline (Glu–Val–Cit) cleavable linker, *p*-aminobenzoyloxycarbonyl (PABC) group, and MMAF (Fig. S2A). MMAF is usually conjugated with maleimide-based non-cleavable linkers based on the general assumption that cleavable valine-citrulline (Val–Cit)-MMAF can undergo premature payload release in circulation prior to reaching target tumors. However, we have uncovered that our branched linker system requires the cleavable Glu–Val–Cit sequence to maximize ADC efficacy *in vivo*(25). Encouragingly, this linker can prevent premature linker degradation in human and mouse plasma. In addition, our conjugation method does not rely on cysteine-maleimide coupling, which is known to undergo deconjugation and loss of payload in circulation(29). These features assure the validity of our ADC design. We obtained homogeneous DAR-4 and DAR-8 ADCs from the mAbs in a quantitative manner. Average DARs of these ADCs were determined to be 4 and 8, respectively (Fig. S2B, C). We also prepared non-targeting ADC as an isotype control constructed using the same payload module (DAR: 4) in the same manner. Size-exclusion chromatography (SEC) analysis showed that both anti-LILRB4 ADCs existed predominantly in the monomer form (Fig. 2B). In addition, no significant aggregation was observed for both ADCs after incubation at 37 °C in PBS for 28 days, demonstrating their long-term thermal stability (Fig. 2C). Hydrophobicity of the ADCs was also assessed by hydrophobic interaction chromatography (HIC) analysis (Fig. 2D). We confirmed that the DAR-8 ADC (26.8 min) was much more hydrophobic than the DAR-4 ADC (retention time: 18.3 min) due to the increased number of hydrophobic MMAF.

In vitro evaluation of the ADCs for LILRB4-dependent binding and cytotoxicity

We determined the binding affinity of the anti-LILRB4 ADCs constructed for recombinant human LILRB4 by ELISA (Fig. S3). Both DAR-4 and -8 ADCs showed similar binding affinity (K_D : 0.16 and 0.21 nM, respectively) to the parental N297A Fc variant (K_D : 0.15 nM). This result indicates that conjugating the branched linker and MMAF components at Q295 (and Q297 in the case of the N297Q mAb) within the Fc region did not impact the LILRB4 antigen binding. This result is consistent with our previous report using anti-HER2 mAbs(25).

We then performed an *in vitro* cytotoxicity assay using three AML cell lines with varying LILRB4 expression levels: THP-1 (AML, LILRB4⁺⁺), MV4-11 (LILRB4⁺), and U937 (LILRB4⁻) (Fig. 3A and Table S1). Live and dead cells were counted by flow cytometry after a 5-day treatment with each conjugate. As anticipated, MMAF alone did not show high potency or target specificity in either cell line. Importantly, both DAR-4 and -8 ADCs could efficiently kill THP-1 and MV4-11 cells. In particular, the DAR-8 ADC exerted much greater potency (EC_{50} : 9.3 pM in THP-1 and 19.7 pM in MV4-11) than the DAR-4 variant (EC_{50} : 25 pM in THP-1 and 374 pM in MV4-11). As expected, the unmodified anti-LILRB4 mAb and a non-targeting ADC prepared from an isotype control (DAR-4) showed a marginal cell killing effect in these LILRB4-positive cells. U937 cells have no detectable LILRB4 expression, and correspondingly, no cytotoxicity was observed following incubation with the DAR-4 ADC, the non-targeting ADC, or the unmodified mAb. The DAR-8 ADC showed moderate cytotoxicity only at very high concentrations (>10 nM). This result suggests that a limited amount of DAR-8 is internalized. We next evaluated the ADCs for potential on-target off-tumor toxicity against CD34⁺ umbilical cord blood cells (UCB-CD34) in a colony-forming unit (CFU) assay (Fig. 3B). There were no differences in the colony number when cells were treated with increased concentrations of the unmodified anti-LILRB4 mAb, DAR-4 ADC or non-targeting ADC whereas the DAR-8 ADC showed moderate toxicity only at very high concentrations (>5,000 ng/mL or >30 nM). None of the treatments had major effects on the contributions of BFU-erythroid (E), CFU-granulocytemonocyte (GM), or CFU-granulocyte-erythroid-monocyte-megakaryocyte (GEMM) colony numbers (Fig. 3C). These results demonstrate that our anti-LILRB4 ADCs, in particular the DAR-4 ADC can selectively kill LILRB4-positive monocytic AML cells while sparing off-target progenitor cells.

In vivo evaluation of the ADCs for PK and therapeutic efficacy

We further evaluated the anti-LILRB4 ADCs in a mouse model of human AML. Seven days after NSG mice received THP cells intravenously, each conjugate was administered at 3 mg/kg via the tail vein. For PK evaluation, blood samples were collected periodically. After extracting serum, we performed sandwich ELISA to determine the serum concentration of total antibody (Fig. 4A and Table S2). The unmodified mAb and the DAR-4 ADC showed comparable clearance rates and areas under the curve (AUC). In contrast, the DAR-8 ADC was cleared at a faster rate, resulting in significantly reduced AUC. This rapid clearance is likely caused by the increased hydrophobicity as seen in the HIC analysis. These results show that the DAR-8 ADC possesses an undesirable PK profile.

Finally, we tested the LILRB4-targeting ADCs for *in vivo* treatment efficacy in a mouse model of human AML. THP-1 cells that stably expressed luciferase were intravenously injected into NSG mice to establish a disseminated AML model. At 7 days post transplantation, each conjugate (3 mg/kg) was administered weekly for the first three weeks (Fig. 4B, C). Both DAR-4 and -8 ADCs exerted therapeutic effect with statistically significant survival benefits (Table S3). Notably, the DAR-8 ADC was inferior to the DAR-4 ADC. The poor PK profile of the DAR-8 ADC may account for the reduced efficacy despite increased DAR. There were no obvious differences in body weight among the mAb and ADC treatment groups (Fig. S4), suggesting that the ADC treatment did not cause significant acute toxicity in this model.

Discussion

Although the anti-CD33 ADC gemtuzumab ozogamicin (Mylotarg[®]) was reapproved in 2017(9), efforts to establish anti-CD33 therapies for AML have been frustrated by the narrow therapeutic indices due to broad expression of CD33 in normal HSCs(30). Indeed, clinical trials for vadastuximab talirine (SGN-CD33A), another anti-CD33 ADC, have recently been discontinued because of increased fatality rates(31). Thus, exploration of novel targets is critically needed to establish ADC-based AML therapies with improved efficacy and safety. CLL-1, a novel AML target, was recently tested in ADC-based efficacy studies(12). An anti-CD123 ADC (IMGN632) is currently in clinical trials for AML treatment(11). However, CD123 is also expressed on normal HSCs, raising safety concerns similar to those for anti-CD33 therapies(30). Indeed, a Phase 1 study for the anti-CD123 ADC SGN-CD123A was unsuccessful and has been terminated because of safety concerns in patients with AML ([NCT02848248](https://clinicaltrials.gov/ct2/show/study/NCT02848248)).

We have been studying the function and signaling of LILRBs in cancer development. We and others have demonstrated that several immunoreceptor tyrosine-based inhibition motif (ITIM)-receptors including LILRB1, LILRB2, LILRB4, and LAIR1 support development of leukemia and other cancers(15,18,19,32–36). Several LILRBs were ranked as AML target candidates(37). Results of our previous studies suggested that LILRBs have dual roles as immune checkpoint molecules and as tumor-sustaining factors(15). In particular, LILRB4 is expressed on monocytic lineages with significantly higher levels of expression on leukemia cells than on normal monocytes, HSCs, or progenitor cells(18,19). In addition to monocytic AML, LILRB4 is known to be expressed in other hematologic malignancies, including 50% of cases of chronic lymphocytic leukemia(38) and some cases of multiple myeloma and MLL-rearranged Pre-B ALL(18,39). Moreover, LILRB4 was reported to be expressed on myeloid-derived suppressor cells(40), tolerogenic dendritic cells(41), and tumor-associated macrophages(15,32), components of the immunosuppressive tumor microenvironment(42–44). Certain solid organ tumors, such as colorectal carcinoma, pancreatic carcinoma, and melanoma, have soluble LILRB4 detected that may inhibit T cell immunity *in vitro*(15). Collectively, these considerations show that LILRB4 represents an ideal target for leukemia therapy with potentially minimal myelotoxicity(18–20).

We have previously identified h-128-3, a human anti-LILRB4 mAb generated by our group, as a potential therapeutic candidate for LILRB4-targeted immunotherapy of AML(19,26).

In addition, our initial evaluation in this report revealed that N297A and N297Q h-128–3 mAbs were efficiently internalized into LILRB4-positive AML cells via endocytosis, an initial step toward ADC target-specific cytotoxicity. Further evaluation will be needed to better understand the kinetics of this LILRB4-mediated endocytosis and the alternation of the expression level after continual treatment with anti-LILRB4 mAbs. Nonetheless, these findings encouraged us to pursue the use of the h-128–3 mAbs in the ADC format for selective delivery of potent chemotherapeutic agents to monocytic AML cells.

We prepared the anti-LILRB4 ADCs from the h-128–3 mAbs with an N297A or N297Q mutation. This mutation allows us to omit the removal of the *N*-glycan chain at N297, a necessary step for our MTGase-mediated antibody–linker conjugation at Q295(45). More importantly, the lack of the *N*-glycan is likely advantageous in terms of ADC toxicity profile. Studies have shown that liver toxicity associated with ADCs is caused by interactions of the antibody glycans with mannose receptors and Fc γ receptor-positive cells, leading to off-target cellular uptake(46). Given the subnanomolar potency of our ADCs in LILRB4-positive cells, the loss of complement-dependent cytotoxicity (CDC), antibody-dependent cellular cytotoxicity (ADCC), and antibody-dependent cellular phagocytosis (ADCP) caused by omission of the *N*-glycan should minimally attenuate the overall *in vivo* efficacy. Together, the use of Fc-mutated anti-LILRB4 ADCs appears to be a practical means to broaden their therapeutic indices.

Using our conjugation technologies, we prepared anti-LILRB4 ADCs with high homogeneity that retained binding affinity to LILRB4. The DAR-8 ADC showed higher hydrophobicity than that of the DAR-4 variant. However, no significant aggregation was observed in either case even after long-term incubation at 37 °C. Both DAR-4 and DAR-8 ADCs exhibited sub-nanomolar-level cell killing potency in LILRB4-positive AML cells (THP-1 and MV11–4) but not in LILRB4 negative cells (U937). As shown in this and other reports, MMAF alone was not capable of killing these cells at such low concentrations because of its poor membrane permeability(47). These results support our hypothesis that the h-128–3 mAb is a good vehicle for drug delivery. In our cell killing assays, the DAR-8 ADC was more than twice as potent as the DAR-4 ADC. The drug multiplicity effect was much more significant in MV4–11 cells expressing LILRB4 at a moderate level rather than in THP-1 with high LILRB4 expression. This result indicates that the number of ADC molecules delivered to THP-1 was close to saturation even at DAR4 because of high LILRB4 expression.

The ADCs were also tested for potential on-target off-tumor toxicity against CD34⁺ umbilical cord blood cells. Our results clearly show that our anti-LILRB4 ADCs can spare off-target progenitor cells. Finally, our LILRB4 ADCs were tested for therapeutic efficacy in a disseminated THP-1 model, a more clinically relevant model than subcutaneous xenograft models. N297A h-128–3 mAb provided a marginal therapeutic effect due largely to lack of Fc-mediated ADCC and ADCP(26). The DAR-4 and DAR-8 conjugates provided 36% and 24% extension of median survival time, respectively. Our prior analysis has shown that the expression level of LILRB4 in patient-derived primary monocytic AML cells is generally higher than that in THP-1 cells(19). Thus, this result indicates that our LILRB4-ADCs could exert a meaningful therapeutic effect in a majority of AML patients. There was no

acute toxicity associated with ADC administration in the mouse model. While encouraging, it has been reported that mice are more resistant to toxicity caused by auristatins than humans(48). Therefore, in-depth studies using advanced models (e.g., humanized mice, primates) are needed to determine the potential toxicity of our ADCs to the human body. In contrast to our observation in the cell-killing assays, the DAR-4 ADC outperformed the DAR-8 variant in the *in vivo* model. Both of our conjugates were constructed using the Glu-Val-Cit linker system with exceptional stability in mouse circulation(25). Considering this point, the rapid clearance of DAR-8 ADC is likely caused by its increased hydrophobicity, in agreement with previous reports on *in vitro* and *in vivo* efficacy of hydrophobic high-DAR ADCs(13,49). Although drug potency is not a negligible contributing factor, this result highlights the critical importance of the PK profile for *in vivo* efficacy. Conjugation technologies that enable the installation of highly potent payloads without exacerbating PK and biodistribution profiles could yield anti-LILRB4 ADCs with improved overall efficacy. One strategy that could allow us to achieve this goal is installation of payloads much more potent than MMAF, for instance tubulysin or pyrrolobenzodiazepine (PBD) dimers. Testing such different payload types is also crucial to better understand payload-associated toxicity profiles (e.g., ocular toxicity caused by MMAF). Another strategy is masking hydrophobic High-DAR ADCs with hydrophilic long chains such as PEG(49) and polysarcosine(50).

We believe LILRB4-targeting ADCs should have only minimal toxicity compared to any other antibody-based agents based on the following reasons. **A)** LILRB4 is only expressed on monocytic cells but not other cells including myeloid progenitors or stem cells (Fig 3B, C). Thus, the toxicity of anti-LILRB4 ADCs will be lower than other anti-AML agents with myeloablative activities. **B)** LILRB4 is much more highly expressed on monocytic AML cells than on normal monocytic counterparts(19). Therefore, our anti-LILRB4 ADCs likely have a poorer ability to kill normal monocytic cells than to monocytic AML cells. **C)** In human, low or high numbers of monocytes do not usually cause symptoms. A reasonable comparison of the potential monocytic cell depletion by our agent can be made for a disorder called the MonoMAC syndrome. MonoMAC is a rare autosomal dominant syndrome associated with monocytopenia, B and NK cell lymphopenia and mycobacterial, fungal and viral infections. In patients with MonoMAC, twelve distinct mutations in the GATA2 gene have been identified, which include missense mutations affecting the zinc finger-2 domain and insertion/deletion mutations leading to frameshifts and premature termination. Because the GATA-2 mutations affect the activity of hematopoietic stem cells and multiple lineages (monocytes, B cells, and NK cells), it is unreasonable to raise a lack of monocytes as the sole factor contributing to microbial and viral infections caused by this disease. Conceptually, one would think B cells and NK cells play more important roles than monocytes in protecting against infections. Even in that scenario, the biomedical and clinical research community has seen the success of the anti-CD20 mAbs Rituximab (Rituxan[®]) as a heme-onc drug and Ocrelizumab (Ocrevus[®]) as a multiple sclerosis drug with manageable adverse effects. Collectively, even if normal monocytic cells are killed by an anti-LILRB4 ADC, the toxicity would be minimal.

In summary, we have demonstrated that targeting LILRB4 using ADCs is a promising strategy for eradicating monocytic AML cells. We expect that fine-tuning several factors,

including the choice of payload and conjugation strategies, will provide more efficacious ADCs than the prototype presented in this study. This study warrants further evaluation of the anti-LILRB4 ADCs in immunocompetent models (e.g., humanized mice), more specifically, the assessment of the synergistic effect derived from its ability of immune checkpoint modulation. It is also important to evaluate these ADCs in more advanced animal models including primates to further validate the clinical translatability. Such efforts may lead to novel drug candidates with the potential to become effective and safe anti-tumor therapy based on targeting LILRB4.

Supplementary Material

Refer to Web version on PubMed Central for supplementary material.

Acknowledgements

We thank Dr. Georgina T. Salazar for editing the manuscript. This work was supported by the National Cancer Institute (1R01CA248736 to C.C.Z.), the Department of Defense (the Breast Cancer Research Program, W81XWH-18-1-0004 and W81XWH-19-1-0598 to K.T.), the Cancer Prevention and Research Institute of Texas (DP150056 and RP180435 to C.C.Z.; RP150551 and RP190561 to Z.A.), the Welch Foundation (AU-0042–20030616 to Z.A.), the University of Texas System (Regents Health Research Scholars Award to K.T.), and the Japan Society for the Promotion of Science (postdoctoral fellowship to Y.A. and A.Y.).

Disclosure of Potential Conflicts of Interest

Patent applications relating to the work filed by the Board of Regents of the University of Texas System are as follows: PCT/US2016/020838, PCT/US2017/044171 (named inventors in both applications: M.D., X.G., N.Z., C.C.Z., and Z.A.), and PCT/US2018/034363 (named inventors: Y.A., C.M.Y., N.Z., Z.A., and K.T.). The first two applications have been exclusively licensed to Immune-Onc Therapeutics by the Board of Regents of the University of Texas System. N.Z., C.C.Z., and Z.A. have a sponsored research agreement with Immune-Onc Therapeutics. C.C.Z. and Z.A. are Scientific Advisory Board members with Immune-Onc Therapeutics. M.D., C.C.Z., and Z.A. own equities of Immune-Onc Therapeutics. A.Y. declares no competing interests.

References

1. Ganzel C, Manola J, Douer D, Rowe JM, Fernandez HF, Paietta EM, et al. Extramedullary Disease in Adult Acute Myeloid Leukemia Is Common but Lacks Independent Significance: Analysis of Patients in ECOG-ACRIN Cancer Research Group Trials, 1980–2008. *J Clin Oncol.* 2016;34:3544–53. [PubMed: 27573652]
2. Röhlig C, Ehninger G. How I treat hyperleukocytosis in acute myeloid leukemia. *Blood.* 2015;125:3246–52. [PubMed: 25778528]
3. Harris AC, Kitko CL, Couriel DR, Braun TM, Choi SW, Magenau J, et al. Extramedullary relapse of acute myeloid leukemia following allogeneic hematopoietic stem cell transplantation: incidence, risk factors and outcomes. *Haematologica.* 2013;98:179–84. [PubMed: 23065502]
4. Lai C, Doucette K, Norsworthy K. Recent drug approvals for acute myeloid leukemia. *J Hematol Oncol.* 2019;12:100. [PubMed: 31533852]
5. DiNardo CD, Pratz K, Pullarkat V, Jonas BA, Arellano M, Becker PS, et al. Venetoclax combined with decitabine or azacitidine in treatment-naïve, elderly patients with acute myeloid leukemia. *Blood.* 2019;133:7–17. [PubMed: 30361262]
6. Bisailon R, Moison C, Thiollier C, Kros J, Bordeleau M-E, Lehnertz B, et al. Genetic characterization of ABT-199 sensitivity in human AML. *Leukemia.* 2020;34:63–74. [PubMed: 31300747]
7. Chau CH, Steeg PS, Figg WD. Antibody–drug conjugates for cancer. *The Lancet.* 2019;394:793–804.
8. Godwin CD, Gale RP, Walter RB. Gemtuzumab ozogamicin in acute myeloid leukemia. *Leukemia.* 2017;31:1855–68. [PubMed: 28607471]

9. Norsworthy KJ, Ko C-W, Lee JE, Liu J, John CS, Przepiora D, et al. FDA Approval Summary: Mylotarg for Treatment of Patients with Relapsed or Refractory CD33-Positive Acute Myeloid Leukemia. *Oncologist*. 2018;23:1103–8. [PubMed: 29650683]
10. Pearce DJ, Taussig DC, Bonnet D. Implications of the expression of myeloid markers on normal and leukemic stem cells. *Cell Cycle*. 2006;5:271–3. [PubMed: 16397415]
11. Kovtun Y, Jones GE, Adams S, Harvey L, Audette CA, Wilhelm A, et al. A CD123-targeting antibody-drug conjugate, IMG632, designed to eradicate AML while sparing normal bone marrow cells. *Blood Adv*. 2018;2:848–58. [PubMed: 29661755]
12. Jiang Y-P, Liu BY, Zheng Q, Panuganti S, Chen R, Zhu J, et al. CLT030, a leukemic stem cell-targeting CLL1 antibody-drug conjugate for treatment of acute myeloid leukemia. *Blood Adv*. 2018;2:1738–49. [PubMed: 30037800]
13. Hamblett KJ, Senter PD, Chace DF, Sun MMC, Lenox J, Cerveny CG, et al. Effects of drug loading on the antitumor activity of a monoclonal antibody drug conjugate. *Clin Cancer Res*. 2004;10:7063–70. [PubMed: 15501986]
14. Li F, Sutherland MK, Yu C, Walter RB, Westendorf L, Valliere-Douglass J, et al. Characterization of SGN-CD123A, A Potent CD123-Directed Antibody-Drug Conjugate for Acute Myeloid Leukemia. *Mol Cancer Ther*. 2018;17:554–64. [PubMed: 29142066]
15. Kang X, Kim J, Deng M, John S, Chen H, Wu G, et al. Inhibitory leukocyte immunoglobulin-like receptors: Immune checkpoint proteins and tumor sustaining factors. *Cell Cycle*. 2016;15:25–40. [PubMed: 26636629]
16. Carosella ED, Rouas-Freiss N, Roux DT-L, Tronik-Le Roux D, Moreau P, LeMaout J. HLA-G: An Immune Checkpoint Molecule. *Adv Immunol*. 2015;127:33–144. [PubMed: 26073983]
17. Inui M, Hirota S, Hirano K, Fujii H, Sugahara-Tobinai A, Ishii T, et al. Human CD43+ B cells are closely related not only to memory B cells phenotypically but also to plasmablasts developmentally in healthy individuals. *Int Immunol*. 2015;27:345–55. [PubMed: 25744616]
18. John S, Chen H, Deng M, Gui X, Wu G, Chen W, et al. A Novel Anti-LILRB4 CAR-T Cell for the Treatment of Monocytic AML. *Mol Ther*. 2018;26:2487–95. [PubMed: 30131301]
19. Deng M, Gui X, Kim J, Xie L, Chen W, Li Z, et al. LILRB4 signalling in leukaemia cells mediates T cell suppression and tumour infiltration. *Nature*. 2018;562:605–9. [PubMed: 30333625]
20. Dobrowolska H, Gill KZ, Serban G, Ivan E, Li Q, Qiao P, et al. Expression of immune inhibitory receptor ILT3 in acute myeloid leukemia with monocytic differentiation. *Cytometry B Clin Cytom*. 2013;84:21–9. [PubMed: 23027709]
21. Anami Y, Xiong W, Gui X, Deng M, Zhang CC, Zhang N, et al. Enzymatic conjugation using branched linkers for constructing homogeneous antibody-drug conjugates with high potency. *Org Biomol Chem*. 2017;15:5635–42. [PubMed: 28649690]
22. Anami Y, Tsuchikama K. Transglutaminase-Mediated Conjugations. *Methods Mol Biol*. 2020;2078:71–82. [PubMed: 31643050]
23. King HD, Yurgaitis D, Willner D, Firestone RA, Yang MB, Lasch SJ, et al. Monoclonal antibody conjugates of doxorubicin prepared with branched linkers: A novel method for increasing the potency of doxorubicin immunoconjugates. *Bioconjugate Chem*. 1999;10:279–88.
24. Yasunaga M, Manabe S, Matsumura Y. New concept of cytotoxic immunoconjugate therapy targeting cancer-induced fibrin clots. *Cancer Sci*. 2011;102:1396–402. [PubMed: 21481097]
25. Anami Y, Yamazaki CM, Xiong W, Gui X, Zhang N, An Z, et al. Glutamic acid-valine-citrulline linkers ensure stability and efficacy of antibody-drug conjugates in mice. *Nat Commun*. 2018;9:2512. [PubMed: 29955061]
26. Gui X, Deng M, Song H, Chen Y, Xie J, Li Z, et al. Disrupting LILRB4/APOE Interaction by an Efficacious Humanized Antibody Reverses T-cell Suppression and Blocks AML Development. *Cancer Immunol Res*. 2019;7:1244–57. [PubMed: 31213474]
27. Reddy N, Ong GL, Behr TM, Sharkey RM, Goldenberg DM, Mattes MJ. Rapid blood clearance of mouse IgG2a and human IgG1 in many nude and nu/+ mouse strains is due to low IgG2a serum concentrations. *Cancer Immunol Immunother*. 1998;46:25–33. [PubMed: 9520289]
28. Cella M, Döhning C, Samaridis J, Dessing M, Brockhaus M, Lanzavecchia A, et al. A novel inhibitory receptor (ILT3) expressed on monocytes, macrophages, and dendritic cells involved in antigen processing. *J Exp Med*. 1997;185:1743–51. [PubMed: 9151699]

29. Lyon RP, Setter JR, Bovee TD, Doronina SO, Hunter JH, Anderson ME, et al. Self-hydrolyzing maleimides improve the stability and pharmacological properties of antibody-drug conjugates. *Nat Biotechnol.* 2014;32:1059–62. [PubMed: 25194818]
30. Taussig DC, Pearce DJ, Simpson C, Rohatiner AZ, Lister TA, Kelly G, et al. Hematopoietic stem cells express multiple myeloid markers: implications for the origin and targeted therapy of acute myeloid leukemia. *Blood.* 2005;106:4086–92. [PubMed: 16131573]
31. Seattle Genetics, Inc. Seattle Genetics Discontinues Phase 3 CASCADE Trial of Vadastuximab Talirine (SGN-CD33A) in Frontline Acute Myeloid Leukemia. Available from: <https://investor.seattlegenetics.com/press-releases/news-details/2017/Seattle-Genetics-Discontinues-Phase-3-CASCADE-Trial-of-Vadastuximab-Talirine-SGN-CD33A-in-Frontline-Acute-Myeloid-Leukemia/default.aspx>, June 19, 2017.
32. Suciú-Foca N, Feirt N, Zhang Q-Y, Vlad G, Liu Z, Lin H, et al. Soluble Ig-like transcript 3 inhibits tumor allograft rejection in humanized SCID mice and T cell responses in cancer patients. *J Immunol.* 2007;178:7432–41. [PubMed: 17513794]
33. Barkal AA, Weiskopf K, Kao KS, Gordon SR, Rosental B, Yiu YY, et al. Engagement of MHC class I by the inhibitory receptor LILRB1 suppresses macrophages and is a target of cancer immunotherapy. *Nat Immunol.* 2018;19:76–84. [PubMed: 29180808]
34. Chen H-M, van der Touw W, Wang YS, Kang K, Mai S, Zhang J, et al. Blocking immunoinhibitory receptor LILRB2 reprograms tumor-associated myeloid cells and promotes antitumor immunity. *J Clin Invest.* 2018;128:5647–62. [PubMed: 30352428]
35. Kang X, Lu Z, Cui C, Deng M, Fan Y, Dong B, et al. The ITIM-containing receptor LAIR1 is essential for acute myeloid leukaemia development. *Nat Cell Biol.* 2015;17:665–77. [PubMed: 25915125]
36. Zhang CC, Fu Y-X. Another way to not get eaten. *Nat Immunol.* 2018;19:6–7. [PubMed: 29242546]
37. Perna F, Berman SH, Soni RK, Mansilla-Soto J, Eyquem J, Hamieh M, et al. Integrating Proteomics and Transcriptomics for Systematic Combinatorial Chimeric Antigen Receptor Therapy of AML. *Cancer Cell.* 2017;32:506–519.e5. [PubMed: 29017060]
38. Colovai AI, Tsao L, Wang S, Lin H, Wang C, Seki T, et al. Expression of inhibitory receptor ILT3 on neoplastic B cells is associated with lymphoid tissue involvement in chronic lymphocytic leukemia. *Cytometry B Clin Cytom.* 2007;72:354–62. [PubMed: 17266150]
39. Armstrong SA, Staunton JE, Silverman LB, Pieters R, Boer den ML, Minden MD, et al. MLL translocations specify a distinct gene expression profile that distinguishes a unique leukemia. *Nat Genet.* 2002;30:41–7. [PubMed: 11731795]
40. de Goeje PL, Bezemer K, Heuvers ME, Dingemans A-MC, Groen HJ, Smit EF, et al. Immunoglobulin-like transcript 3 is expressed by myeloid-derived suppressor cells and correlates with survival in patients with non-small cell lung cancer. *Oncoimmunology.* 2015;4:e1014242. [PubMed: 26140237]
41. Chang CC, Ciubotariu R, Manavalan JS, Yuan J, Colovai AI, Piazza F, et al. Tolerization of dendritic cells by T(S) cells: the crucial role of inhibitory receptors ILT3 and ILT4. *Nat Immunol.* 2002;3:237–43. [PubMed: 11875462]
42. Brenk M, Scheler M, Koch S, Neumann J, Takikawa O, Häcker G, et al. Tryptophan deprivation induces inhibitory receptors ILT3 and ILT4 on dendritic cells favoring the induction of human CD4+CD25+ Foxp3+ T regulatory cells. *J Immunol.* 2009;183:145–54. [PubMed: 19535644]
43. Ge G, Tian P, Liu H, Zheng J, Fan X, Ding C, et al. Induction of CD4+ CD25+ Foxp3+ T regulatory cells by dendritic cells derived from ILT3 lentivirus-transduced human CD34+ cells. *Transpl Immunol.* 2012;26:19–26. [PubMed: 22005288]
44. Andersen MH. The targeting of immunosuppressive mechanisms in hematological malignancies. *Leukemia.* 2014;28:1784–92. [PubMed: 24691076]
45. Jeger S, Zimmermann K, Blanc A, Grünberg J, Honer M, Hunziker P, et al. Site-specific and stoichiometric modification of antibodies by bacterial transglutaminase. *Angew Chem Int Ed.* 2010;49:9995–7.

46. Gorovits B, Krinos-Fiorotti C. Proposed mechanism of off-target toxicity for antibody-drug conjugates driven by mannose receptor uptake. *Cancer Immunol Immunother.* 2013;62:217–23. [PubMed: 23223907]
47. Doronina SO, Mendelsohn BA, Bovee TD, Cerveny CG, Alley SC, Meyer DL, et al. Enhanced activity of monomethylauristatin F through monoclonal antibody delivery: effects of linker technology on efficacy and toxicity. *Bioconjugate Chem.* 2006;17:114–24.
48. Mirsalis JC, Schindler-Horvat J, Hill JR, Tomaszewski JE, Donohue SJ, Tyson CA. Toxicity of dolastatin 10 in mice, rats and dogs and its clinical relevance. *Cancer Chemother Pharmacol.* 1999;44:395–402. [PubMed: 10501913]
49. Lyon RP, Bovee TD, Doronina SO, Burke PJ, Hunter JH, Neff-LaFord HD, et al. Reducing hydrophobicity of homogeneous antibody-drug conjugates improves pharmacokinetics and therapeutic index. *Nat Biotechnol.* 2015;33:733–5. [PubMed: 26076429]
50. Viricel W, Fournet G, Beaumel S, Perrial E, Papot S, Dumontet C, et al. Monodisperse polysarcosine-based highly-loaded antibody-drug conjugates. *Chem Sci.* 2019;10:4048–53. [PubMed: 31015945]

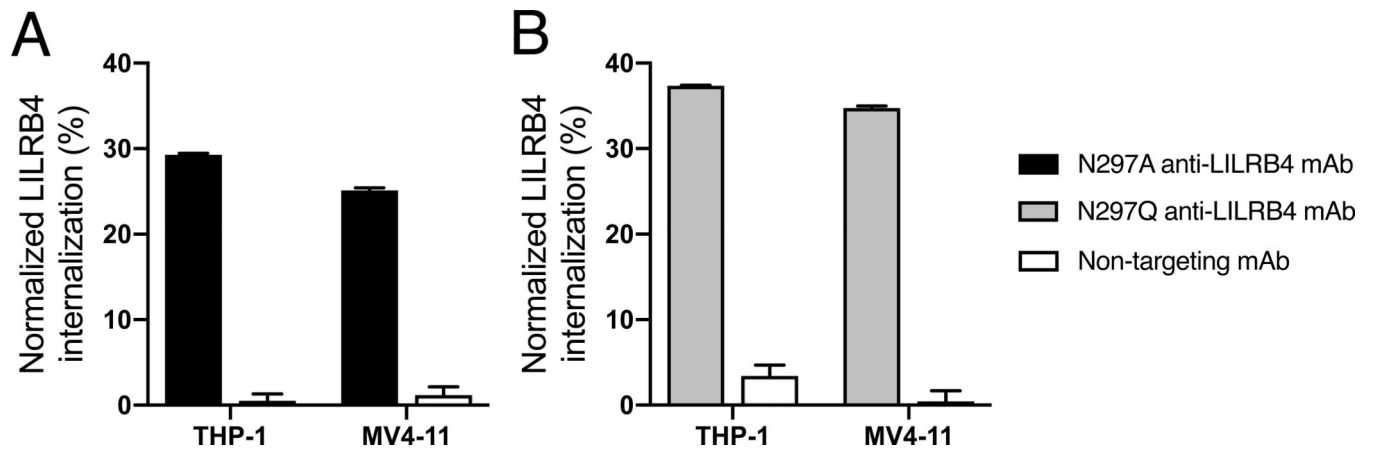
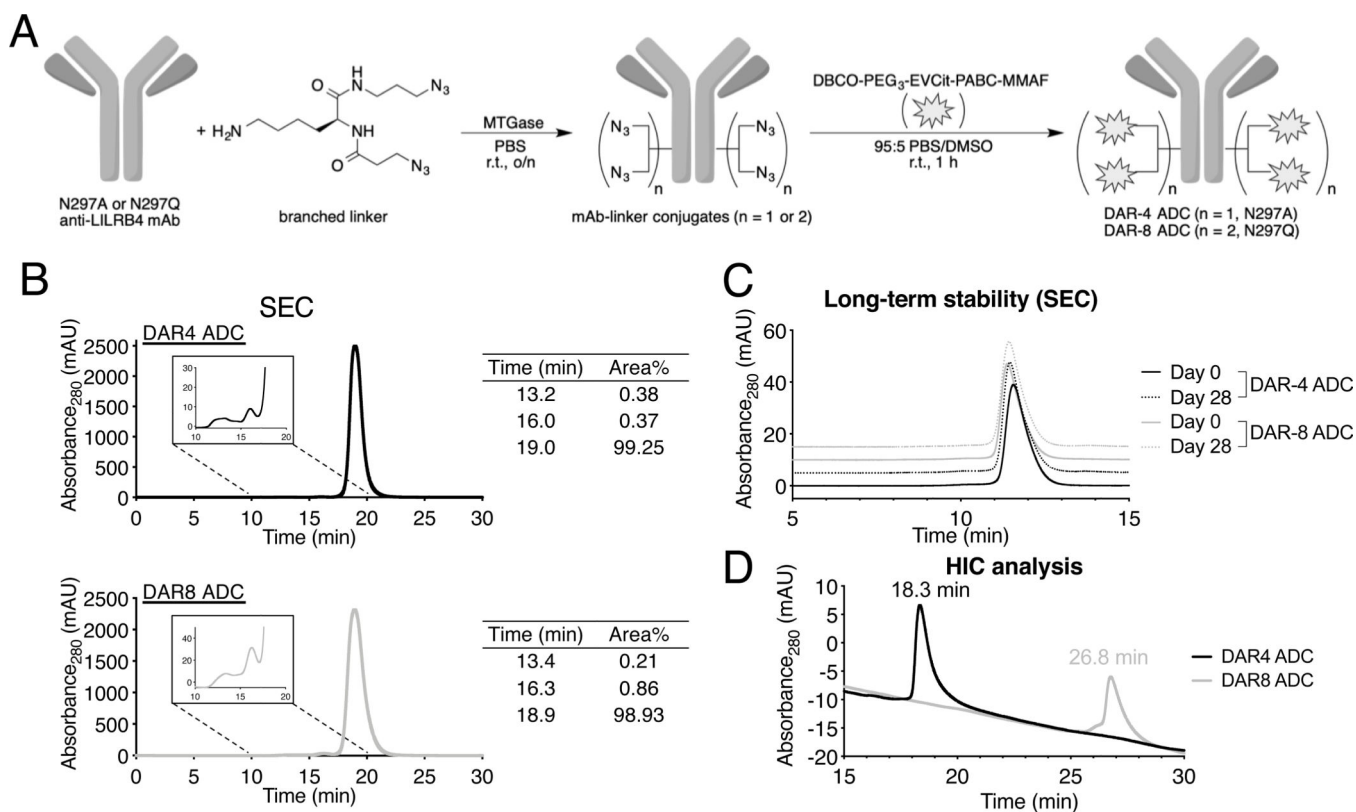


Fig. 1. Internalization of anti-LILRB4 mAb–surface LILRB4 complex. THP-1 and MV4-11 cells were treated with anti-LILRB4 Fc variants with (A) N297A (black) or (B) N297Q mutation (gray) at 37 °C for 24 h before surface LILRB4 was quantified by FACS. A non-targeting mAb (white) was also tested in each assay. The degree of internalization is normalized to the expression level of surface LILRB4 treated with PBS. All assays were performed in duplicate. Error bars represent mean \pm SEM.

**Fig. 2.**

Construction and characterization of homogeneous anti-LILRB4 ADCs. **(A)** Construction of DAR-4 and DAR-8 ADCs by MTGase-mediated branched linker conjugation and following strain-promoted azide–alkyne cycloaddition (spark: DBCO–PEG₃–EVCit–PABC–MMAF module). **(B)** Preparative SEC traces of DAR-4 and DAR-8 ADCs. **(C)** Analytical SEC traces of DAR-4 and DAR-8 ADCs after incubation in PBS at 37 °C for 28 days. **(D)** HIC analysis under physiological conditions (phosphate buffer, pH 7.4). DBCO, dibenzocyclooctyne, EVCit, glutamic acid–valine–citrulline; MTGase, microbial transglutaminase; SEC, size-exclusion chromatography, PABC, *p*-aminobenzyloxycarbonyl; PEG, polyethylene glycol.

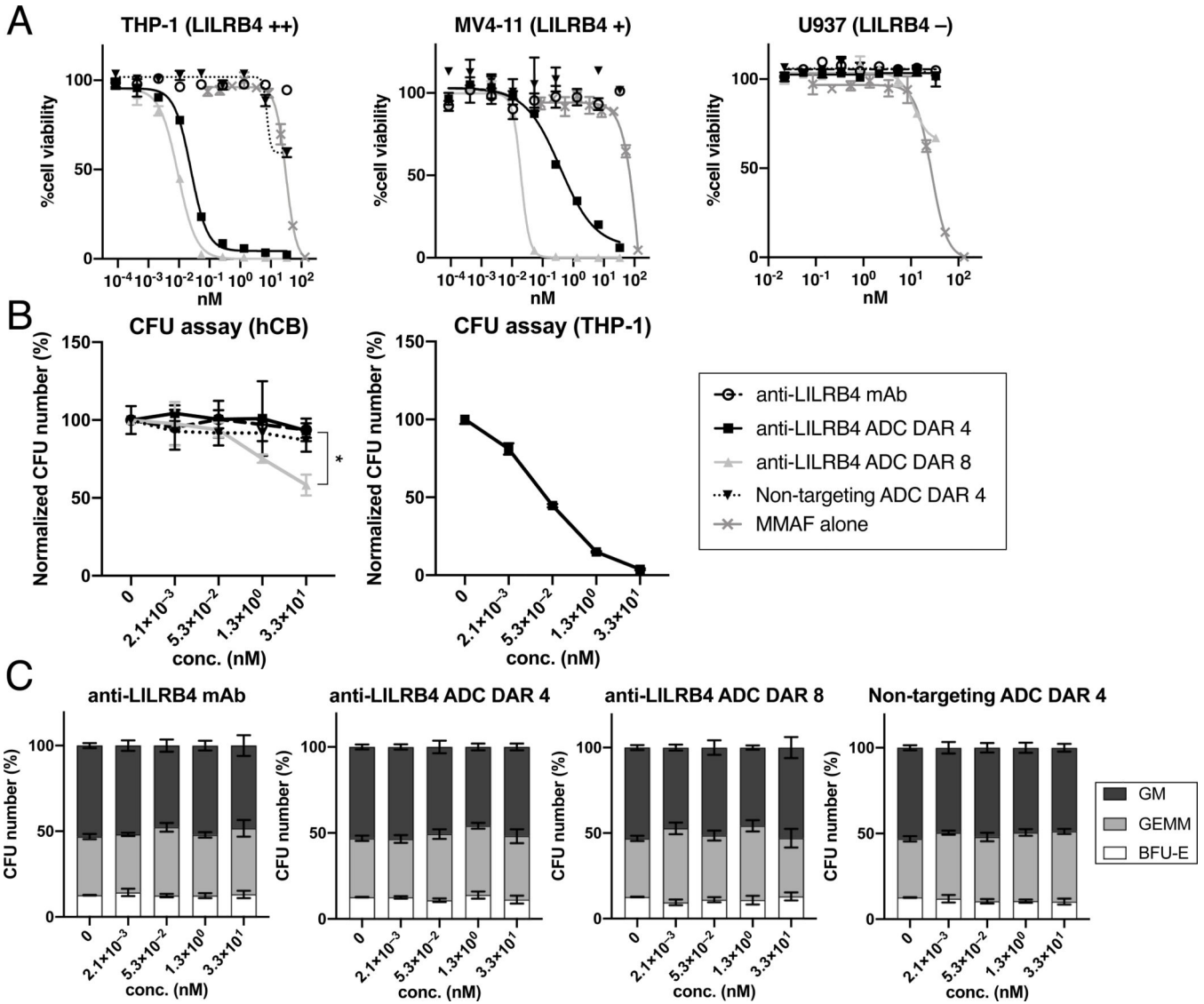


Fig. 3. In vitro cytotoxicity of anti-LILRB4 mAb h128–3, DAR-4 ADC, DAR-8 ADC, and non-targeting DAR-4 ADC (isotype control). (A) Cell killing potency in the AML cell lines THP-1, MV4–11, and U937. (B) CFU assay in THP-1 or CD34⁺ umbilical cord blood cells (UCB-CD34). (C) CFU numbers of BFU-erythroid (E, white), CFU-granulocyte-erythroid-monocyte-megakaryocyte (GEMM, light gray), and CFU-granulocytomonocyte (GM, dark gray) after being treated with each mAb or ADC. CFU numbers are normalized to the count of a untreated group. All assays were performed in triplicate. Error bars represent mean ± SEM. * *P* < 0.05 (DAR 4 vs DAR 8 in hCB, Welch’s *t* test). CFU, colony-forming unit. hCB, human cord blood.

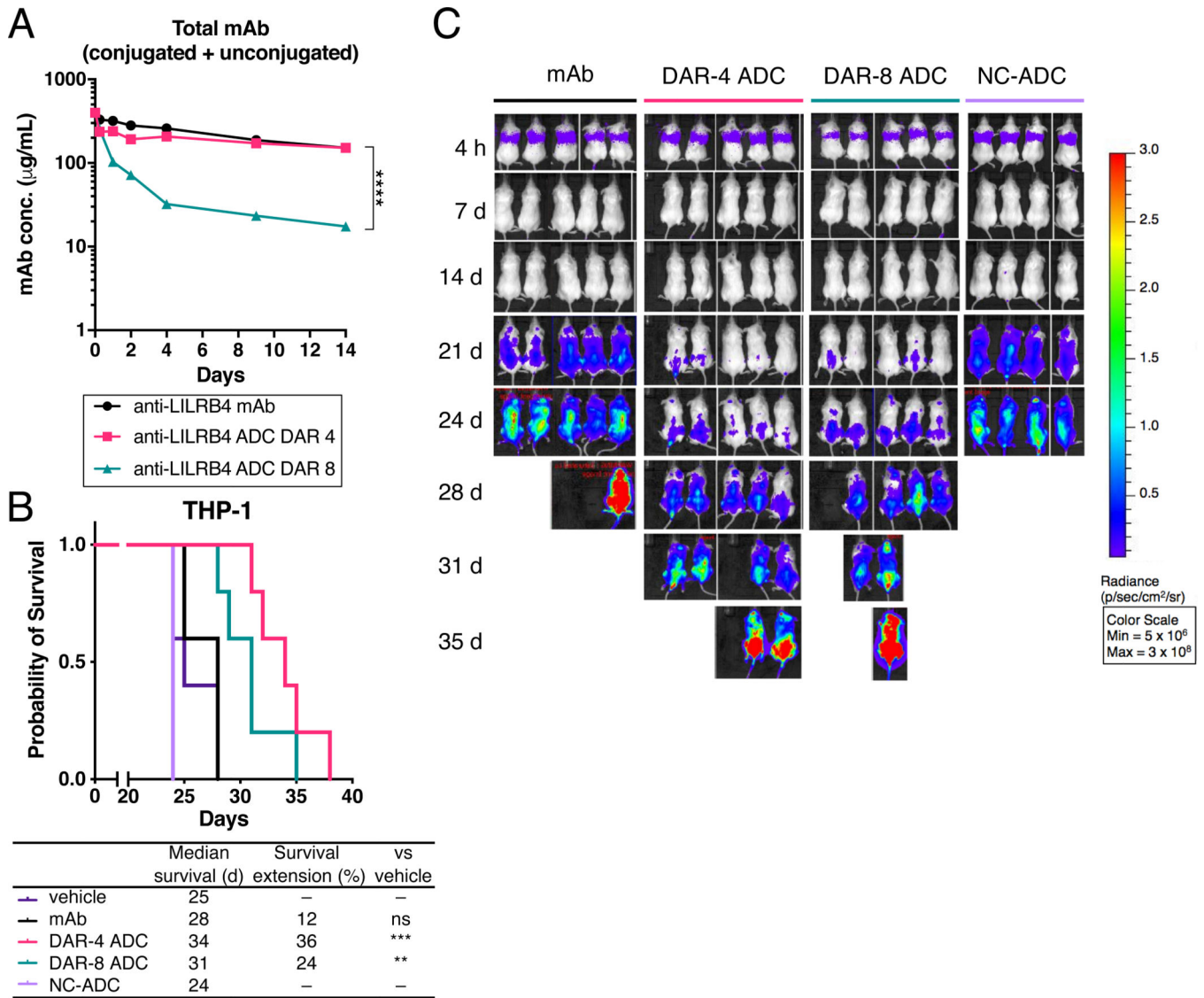


Fig. 4. In vivo evaluation of anti-LILRB4 ADCs. (A) PK of unmodified anti-LILRB4 mAb (black), DAR-4 ADC (magenta), and DAR-8 ADC (green) in female NSG mice ($n = 5$). Mice were injected with each drug at 3 mg/kg. At the indicated time points, blood was collected to quantify total antibody (conjugated and unconjugated) by sandwich ELISA. (B) Kaplan-Meier curve and (C) bioluminescence images of the THP-1 xenograft mouse model (female NSG mice), $n = 4$ for non-targeting control ADC (NC-ADC); $n = 5$ for the other groups. Mice were injected intravenously with THP-1 (1×10^6 cells) on Day 0 and treated with each drug (3 mg/kg) or vehicle control (purple) on Day 7, 14, and 21. ** $P < 0.01$, *** $P < 0.005$, **** $P < 0.0001$ (DAR 4 vs DAR 8 in PK analysis: Welch's t test; survival curve: long rank test).